

1 **Supporting Information of “Generation of skyrmions by combining thermal and spin-**  
2 **orbit torque: breaking half skyrmions to skyrmions”**

3 *Sheng Yang,<sup>#,1</sup> Laichuan Shen,<sup>#,2,3</sup> Yuelel Zhao,<sup>#,1</sup> Kai Wu,<sup>1</sup> Xiaoguang Li,<sup>4</sup> Ka Shen,<sup>2,3</sup> Senfu*  
4 *Zhang,<sup>5</sup> Xiaohong Xu,<sup>6,7</sup> Johan Åkerman<sup>8,9</sup> and Yan Zhou<sup>\*,1</sup>*

5 *<sup>1</sup>School of Science and Engineering, The Chinese University of Hong Kong, Shenzhen, 518172,*  
6 *China*

7 *<sup>2</sup>The Center for Advanced Quantum Studies and Department of Physics, Beijing Normal*  
8 *University, Beijing, 100875, China*

9 *<sup>3</sup>Key Laboratory of Multi-scale Spin Physics, Ministry of Education, Beijing Normal*  
10 *University, Beijing, 100875, China*

11 *<sup>4</sup>Center for Advanced Material Diagnostic Technology, College of Engineering Physics,*  
12 *Shenzhen Technology University, Shenzhen, 518118, China*

13 *<sup>5</sup>Key Laboratory for Magnetism and Magnetic Materials of the Ministry of Education, Lanzhou*  
14 *University, Lanzhou, 730000, China*

15 *<sup>6</sup>School of Chemistry and Materials Science of Shanxi Normal University & Key Laboratory*  
16 *of Magnetic Molecules and Magnetic Information Materials of Ministry of Education, Taiyuan,*  
17 *030006, China*

18 *<sup>7</sup>Research Institute of Materials Science of Shanxi Normal University & Collaborative*  
19 *Innovation Center for Shanxi Advanced Permanent Magnetic Materials and Technology,*  
20 *Taiyuan, 030006, China*

21 *<sup>8</sup>Department of Physics, University of Gothenburg, Gothenburg, 41296, Sweden*

22 <sup>9</sup>*Science and Innovation in Spintronics Research Institute of Electrical Communication,*

23 *Tohoku University, Aoba-ku, 980-8577, Japan*

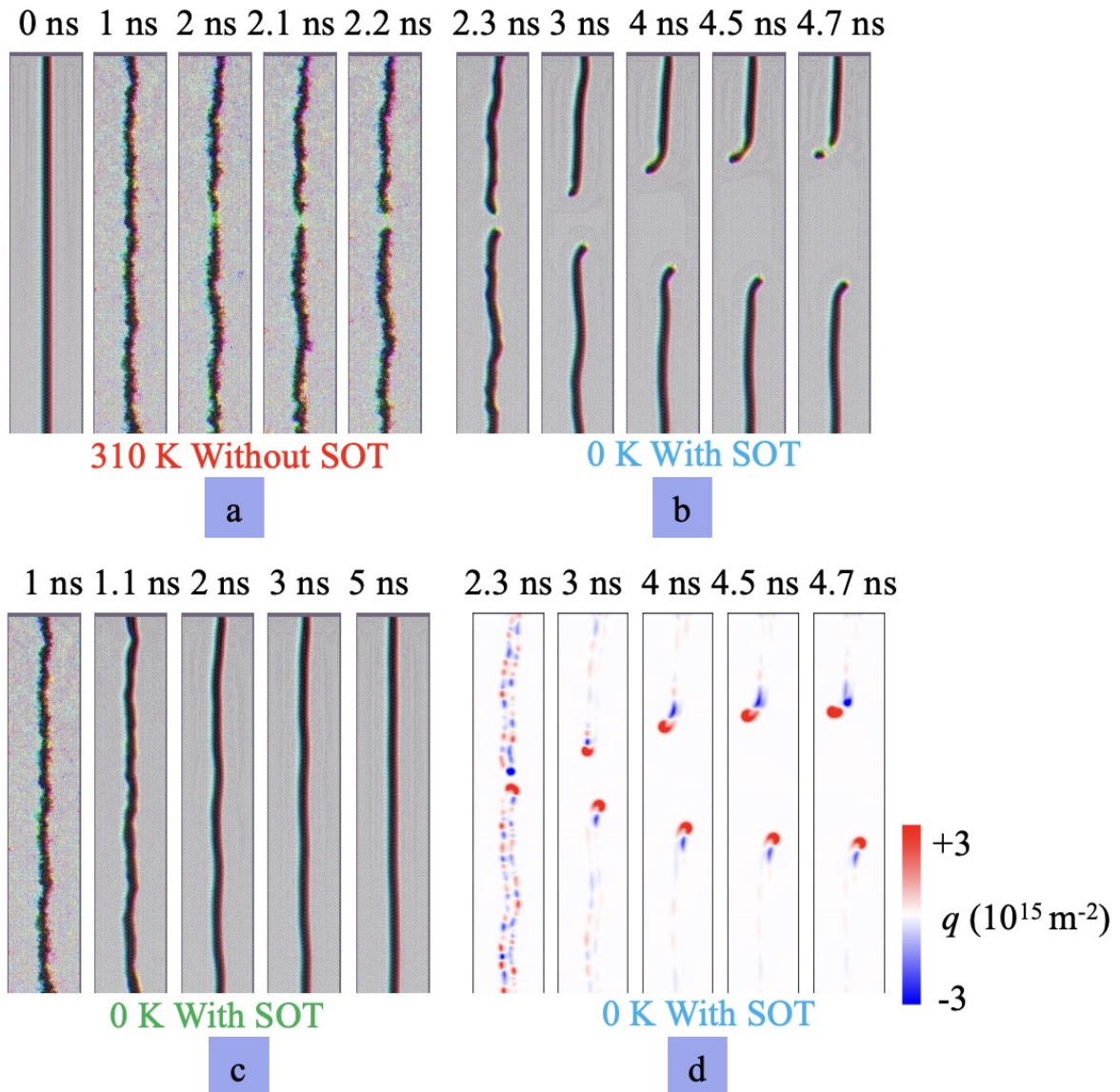
24 **#These authors contributed equally.**

25 **Corresponding Author**

26 \* E-mail: [zhouyan@cuhk.edu.cn](mailto:zhouyan@cuhk.edu.cn)

27

28 Supporting Information S1: Evolution of a single stripe domain



29

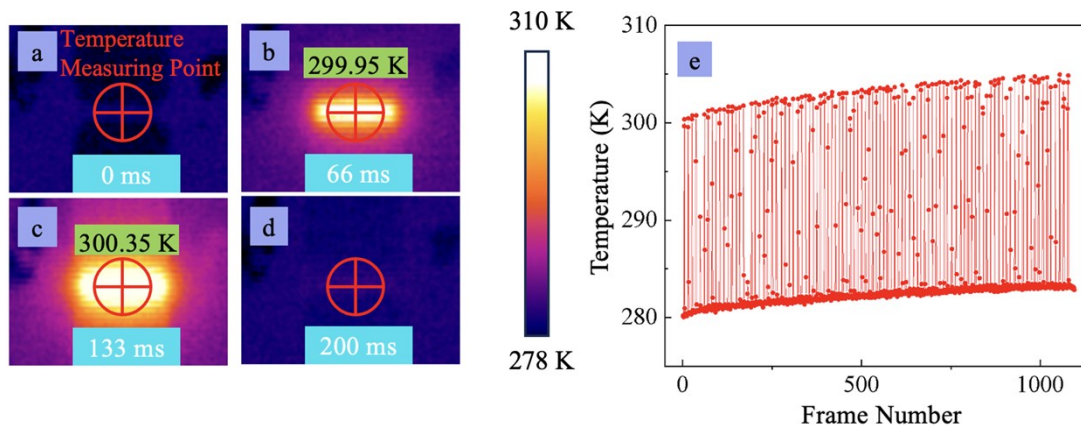
30 Figure S1. Effects of SOT and heat on a single stripe domain. **a.** Heat causes the stripe domain  
 31 to curl and split into two segments. **b.** Under the application of SOT, a skyrmion is cut from  
 32 the end of the split stripe domain. **c.** SOT can restore the straightness of the stripe domain in  
 33 the absence of heat. **d.** The topological density map of **b.** The heat creates the non-uniform  
 34 topological density and varies the spin configuration along the stripe domain.

35

36 Figure S1a shows the time evolution of a single stripe domain under thermal effects at  
 37 310 K. As one can see, such a domain is split into two segments. Then, we set the temperature  
 38 to 0 K and turn on the SOT. As shown in Figure S1b, a skyrmion is generated from the end of  
 39 a split domain, where the distribution of the topological density  $q$  is plotted in Figure S1d,  
 40 confirming the existence of skyrmion. This result indicates that the SOT has a significant  
 41 impact on the transition of stripe domains into skyrmions. It is noteworthy that unlike the  
 42 thermal effect, the SOT cannot break the single stripe domain, as shown in Figure S1c.

43

44 Supporting Information S2: Temperature measurement



45

46 Figure S2. A demonstration of the infrared camera image of the heated device. **a-d**. The  
 47 snapshot of the heated device at time 0 ms, 66 ms, 133 ms, and 200 ms. The position of the  
 48 temperature measurement is manually chosen and positioned at the central point of the track.  
 49 **e**. The plot of temperature vs. frame number of the infrared camera.

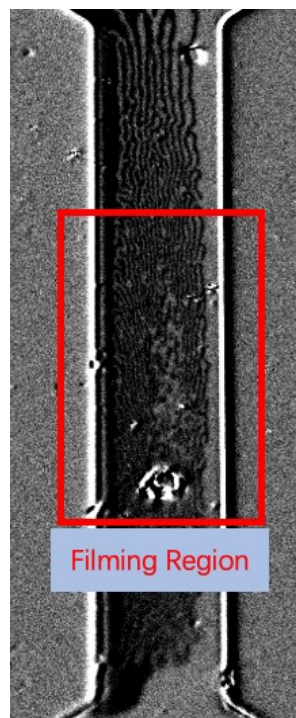
50

51 Figures S2a-d demonstrate the temperature changes measured by the infrared camera of  
 52 our racetrack device under the stimulation of currents. The device has an initial temperature of  
 53 280.15 K (Figure S2a) and is subjected to a current pulse with a density of  $2.40 \times 10^{11}$  A/m<sup>2</sup> and  
 54 a duration of 100 ms. The temperature rises to 299.95K at 66 ms and to 300.35K at 133 ms  
 55 (Figures S2d-c). Following the pulse, the device undergoes a cooling process, yet it remains at

56 a considerably elevated temperature relative to the initial state. The device In Figure S2e, the  
57 temperature of the device measured by the infrared camera increases from 280.15 K to 299.00  
58 K after the first current pulse, and after 100 pulses (current density of  $2.40 \times 10^{11}$  A/m<sup>2</sup> and  
59 width of 100 ms), the temperature of the device reaches 304.85 K. Finally, the temperature  
60 drops to 284.15 K when the pulses ceased. Nevertheless, the device's dimensions are  
61 excessively diminutive for the infrared camera to accurately gauge the temperature at the center  
62 of the device ( or the “hot spot”). Consequently, the precise temperature at the specific site  
63 responsible for the transition between stripe domains and skyrmions remains unsure.

64

65 Supporting Information S3: Filming region of the racetrack device



66

67 Figure S3. Filming region of the racetrack device.

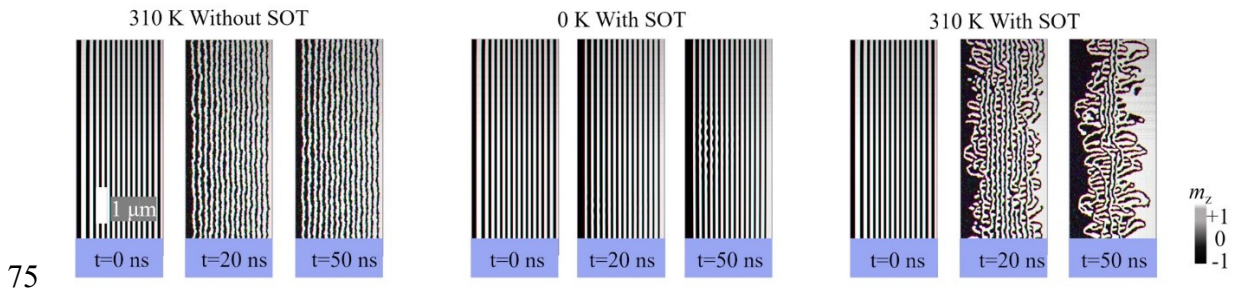
68

69 As shown in Figure S3, the area of maximum temperature, or the “hot spot,” is located at  
70 the center of the racetrack device, where the electrical current distribution is more concentrated,

71 resulting in higher Joule heating. Therefore, the stripe domain – skyrmion transition is first  
72 occurred in the center of the device.

73

74 Supporting Information S4: Domain evolution for a  $2400\text{ nm}\times 6000\text{ nm}\times 1\text{ nm}$  film



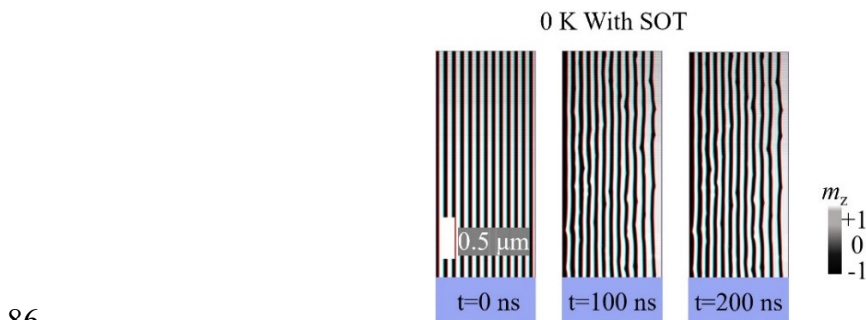
76 Figure S4. Snapshot of magnetic domains of a  $2400\text{ nm}\times 6000\text{ nm}\times 1\text{ nm}$  film at simulation  
77 time 0, 20 and 50 ns, with three scenarios (with/without the SOT at different temperatures).  
78 Other parameters are the same as those used in Figure 4 of the main text.

79

80 In Figure 4 of the main text, the model size is  $1200\text{ nm}\times 3000\text{ nm}\times 1\text{ nm}$ . Its increase does  
81 not give a qualitative change, but only introduce a quantitative modification in the evolution of  
82 magnetic domains, as shown in Figure S4.

83

84 Supporting Information S5: Evolution of magnetic domains driven by spin-orbit torques in  
85 the presence of defects



87 Figure S5. Snapshot of the magnetic domains at different simulation times in the presence of  
88 spin-orbit torques and defects. The parameters are the same as those used in Figure 4 of the  
89 main text.

90

91 Figure S5 shows the time evolution of the magnetic domains driven by spin-orbit torques  
92 in the presence of defects, modeled by randomly modifying the magnetic anisotropy within the  
93 range of  $0.6 \text{ MJ/m}^3 - 0.8 \text{ MJ/m}^3$ . As seen, considering only spin-orbit torque as the driving  
94 source, the introduction of defects into the magnetic film does not give rise to a magnetic state  
95 similar to that presented in Figure 4u, even after 200 ns (a very long simulation time).